Chemical Physics Letters

Aggregation-induced emission of a Eu(III) complex via ligand-to-metal charge transfer

Yuichi Kitagawa,*[ac] Marina Kumagai,[b] Koji Fushimi,[a] and Yasuchika Hasegawa*[,ac]

[a]Faculty of Engineering, Hokkaido University, N13W8, Kita-ku, Sapporo, Hokkaido 060-8628, Japan

[b]Graduate School of Chemical Sciences and Engineering, Hokkaido University, N13W8, Kita-ku, Sapporo, Hokkaido 060-8628, Japan

[c]Institute for Chemical Reaction Design and Discovery (WPI-ICReDD), Hokkaido University, N21W10, Kita-ku, Sapporo, Hokkaido 001-0021, Japan.

Corresponding author footnote:

Tel. /Fax: +81 11 706 7114.

E-mail: y-kitagawa@eng.hokudai.ac.jp (Yuichi Kitagawa)

hasegaway@eng.hokudai.ac.jp (Yasuchika Hasegawa)

Abstract

Aggregation-induced emission (AIE) of a Eu(III) complex using ligand-to-metal charge transfer band is demonstrated. The Eu(III) complex comprises three anionic 2,2,6,6-tetramethyl-3,5-heptanedionate (tmh) ligands and one large π-conjugated neutral dipyrido[3,2-f:2',3'-h]quinoxaline (dpq) ligand. Crystalline H-aggregates of the Eu(III) complex were characterized by X-ray crystal structure analysis. H-aggregation-induced emission (H-AIE) properties were evaluated using emission spectra, emission lifetime, and quantum yields. The energy transfer efficiency of the H-aggregate in the solid state is five times larger than that of the isolated Eu(III) complex in solution.

Introduction

In 2001, Tang and co-workers discovered that a pentaphenylsilole fluorophore was nearly non-emissive in dilute solution but exhibited intense emission in the aggregate state, which was coined aggregation-induced emission (AIE) [1]. This photophysical phenomenon is based on rotational restriction in organic structures resulting from aggregation. Since then, numerous AIE luminophores with strong emission properties have been reported [2-7]. Various AIE luminophore designs, including excited state level modulation, have been studied, expanding the fields of photochemistry and photophysics [8-10].

Zhao employed aggregation-induced thermally activated delayed fluorescence (AI-TADF) to develop an efficient organic light-emitting diode (OLED) [8]. The AIE mechanism relates to the

energies of the ligand-to-ligand charge transfer (LLCT) band. Huang demonstrated that precise control of electronic structure can alter the color of AI-TADF luminescence through changes in aggregation morphology [9]. Recently, our group has observed AIE from 4f-4f transitions in a Tb(III) complex. AIE was ascribed to modulation of the LLCT quenching state by J-aggregation [10]. In contrast, the H-aggregates do not emit a photon because the T_1 level is lower than the emitting level of Tb(III) ion. The H-aggregate triplet state exhibits a long excited lifetime [11-14], which makes it a promising energy donor. In this study, we demonstrate H-aggregation induced emission (H-AIE) of a Eu(III) complex in a solid (crystalline) state using ligand-to-metal charge transfer (LMCT) quench states for the first time.

To prepare a Eu(III) complex with LMCT quench states, we selected the 2,2,6,6-tetramethyl-3,5-heptanedionate ligand. This ligand provides strong, photosensitized energy transfer quenching (photosensitized energy transfer efficiency: $\eta_{sens} < 1.0\%$), which weakened emission intensity [15-17]. Dipyrido[3,2-f:2',3'-h]quinoxaline (dpq) was selected as the energy donor since the large π-conjugated dpq ligand promotes the formation of H-aggregates [10]. The H-aggregation allows for drastic stabilization of the T_1 level by solidification (Figure 1). The solid H-aggregates with a stabilized T_1 state allow the Eu(III) complex to exhibit effective photosensitized emission, although the Eu(III) complex does not emit photons. The H-AIE mechanism differs from that of Tb(III) complexes using LLCT band modulation. Thus, H-AIE via LMCT in lanthanide complexes presents a new frontier for molecular photochemistry and photophysics.

Results and Discussion

Crystal Structure

A single crystal of Eu(tmh)$_3$dpq was obtained by recrystallization from a CH_2Cl_2/hexane solution. The crystal structure of Eu(tmh)$_3$dpq (CCDC:1977232) is shown in Figure 2a. The coordination site of Eu(tmh)$_3$dpq comprises three tmh and one dpq ligands. The bond lengths between the dpq ligand and the Eu(III) ion is longer than those between the tmh ligands and the Eu(III) ion (Table S2). To clarify the polyhedral structure, we calculated continuous shape measures. The continuous shape measure factor, *S,* was calculated to estimate the degree of distortion in the first coordination sphere of the coordination structure based on the crystal structure data [18]. The S value is given by the following equation,

$$S = \min \frac{\sum_k^N \left| Q_k - P_k \right|^2}{\sum_k^N \left| Q_k - Q_o \right|^2} \times 100,$$

where Q_k represents the vertices of the actual structure, Q_0 is the center of mass of the actual structure, N is the number of vertices, and P_k represents the vertices of the ideal structure. The octacoordinated lanthanide complex exhibit square antiprismatic (SAP, point group: D_{4d}), trigonal dodecahedral (TDH, point group: D_{2d}), or biaugmented trigonal prismatic (BTP, point group: C_{2v}) structure according to the *S* value. Based on the shape measure calculation, Eu(tmh)$_3$dpq was categorized as having SAP coordination geometry (*S* = 0.562, Table S6). Strong intermolecular π-π interactions (0.3 nm) between dpq ligands were observed in the crystal structure; these correspond to H-aggregates (Figure 2b). Thus, the crystal structure of Eu(tmh)$_3$dpq demonstrates formation of

H-aggregates in the solid state.

Photophysical properties

Electronic absorption spectra of Tb(tmh)$_3$dpq and Eu(tmh)$_3$dpq in CH_2Cl_2 (1.0×10^{-2} M) are shown in Figure 3. We estimated the onset of absorption band as the absorption edges. The absorption edge of the Tb(III) complex is estimated to be 497 nm (20,120 cm^{-1}), which is assigned as LLCT from the tmh ligands to the dpq ligand [10]. A strongly red-shifted absorption edge is observed in the Eu(III) complex (697 nm (14,340 cm^{-1})). This characteristic absorption band indicates LMCT from the tmh ligand to the Eu(III) ion in the visible light region [15]. Using estimates from solid states, reflection spectra of the H-aggregates were also measured (Figure 4). The absorption bands of the Tb(III) and Eu(III) complexes are observed at around 350 nm and assigned to ligand π–π* transitions. The absorption edges of the Tb(III)- and Eu(III)-based H-aggregates are estimated to be 472 nm (21,200 cm^{-1}) and 510 nm (19,610 cm^{-1}), respectively. H-aggregation induced a large blue-shift in the LMCT band for the Eu(III) complex, while effective energy shift was not observed for the LLCT band in the Tb(III) complex. From these findings, we confirm that H-aggregation strongly affects the LMCT energy level.

The emission spectra of Eu(tmh)$_3$dpq in CH_2Cl_2 (5.0×10^{-2} M, black line) and its H-aggregate (red line) are shown in Figure 5. Emission peaks are observed at 578, 592, 613, 654, and 699 nm; these are assigned to $^5D_0 \rightarrow {}^7F_0$, $^5D_0 \rightarrow {}^7F_1$, $^5D_0 \rightarrow {}^7F_2$, $^5D_0 \rightarrow {}^7F_3$, and $^5D_0 \rightarrow {}^7F_4$ transitions, respectively. The spectrum of isolated Eu(tmh)$_3$dpq in solution differs in shape from that of the H-aggregates in solid

states. This result suggests that LMCT energy level depends on the coordination geometry of the Eu(III) ion. The time-resolved emission profiles of the Eu(III) complexes revealed single exponential decays with lifetimes on the scale of milliseconds (Figure 6).

The photophysical properties of Eu(III) complexes in solution and the solid state are summarized in Table 1. $Eu(tmh)_3dpq$ in CH_2Cl_2 exhibited a high intrinsic luminescence quantum yield (Φ_{ff} = 61%), on par with a previously reported highly luminescent Eu(III) complex [20]. This large Φ_{ff} originates from a large radiative rate constant (k_r = 8.0 × 10^2 s^{-1}) and a small non-radiative rate constant (k_{nr} =5.2 × 10^2 s^{-1}). Emission quantum yields from ligand excitation (Φ_{tot} = 1.2%) are much smaller than Φ_{ff}, due to small photosensitized energy efficiency resulting from LMCT quenching (η_{sens} = 2.0%). Eu(III)-H-aggregates also display relatively large intrinsic luminescence quantum yields (54%), based on their large k_r (7.5 × 10^2 s^{-1}) and small k_{nr} (6.4 × 10^2 s^{-1}) values. Eu(III) H-aggregates exhibited effective photosensitized energy transfer (> 10%). This energy transfer efficiency allows the emission quantum yield of the solid state to be five times larger than that of the solution.

In order to clarify the mechanism of AIE, we estimated the T_1 level from the phosphorescence of the isolated Gd(III) complex in solution and Gd(III) H-aggregates in the solid state [10, 21-22]. Phosphorescence was observed at room temperature for the Gd(III) H-aggregates, while the isolated Gd(III) complex only phosphoresced at low temperature (185 K). Using spectral fitting, the T_1 energy levels of the isolated $Eu(tmh)_3dpq$ complex (Figure S6) and H-aggregates (Figure S7) are estimated to be 20,530 and 17,900 cm^{-1}, respectively. Previously, various Eu(III) complexes with

tmh ligand and various coordination geometry have been showed quite low η_{sens} (< 1.0%). From these results, the H-aggregation induces the low T_1 level energy; this modulation of energy levels results in the observed H-AIE. Thus, we have successfully demonstrated H-AIE via control of LMCT quenching by triplet level modulation in a Eu(III) complex. The energy-accepting state of the T_1 state in the H-aggregates (T_1: 17,900 cm^{-1}) corresponds to the $^5D_0$ level of the Eu(III) ion ($^5D_0$: 17,200 cm^{-1}) because of the large energy gap between the T_1 and $^5D_1$ level of the Eu(III) ion ($^5D_1$: 19,000 cm^{-1}) [19]. A direct energy transfer from the T_1 level to $^5D_0$ level is forbidden, but the energy transfer can be induced by perturbation and thermal population of the $^7F_1$ level [23]. The photosensitized design of a complex with a longer T_1 lifetime allows effective energy transfer from the T_1 level to $^5D_0$ level [24]. We will continue to study novel Eu(III) complexes in an effort to construct more effective H-AIE materials.

Conclusion

In this paper, LMCT quench states in a novel Eu(III) complex were employed to induce H-AIE. The H-aggregation-induced modulation of the energy level of the T_1 state and the LMCT quench states allows a large change in the energy transfer efficiency from the T_1 level to $^5D_0$ level of the Eu(III) ion. Our design for Eu(III)-based H-AIE materials creates a new field at the interface of photophysics and supramolecular chemistry.

Acknowledgment

We are particularly grateful for experimental assistance by Professor H. Ito and Assistant Professor T. Seki of Hokkaido University. This work was supported by Grant-in-Aid for Grant Number 17K14467, 19H04556, 18H04497 and 18H02041. This work was also supported by the Institute for Chemical Reaction Design and Discovery (ICReDD), established by the World Premier International Research Initiative (WPI) of MEXT, Japan. This study was supported in part by Grants-in-Aids for regional R&D Proposal-Based Program from Northern Advancement Center for Science & Technology of Hokkaido, Japan.

Notes and references

[1] J. Luo, Z. Xie, J. W. Y. Lam, L. Cheng, H. Chen, C. Qiu, H. S. Kwok, X. Zhan, Y. Liu, D. Zhu, B. Z. Tang, Chem. Commun. (2001) 1740.

[2] X. Liang, Z.-L. Tu and Y.-X. Zheng, Chem. Eur. J. 25 (2019) 5623..

[3] H.-T. Feng, Y.-X. Yuan, J.-B. Xiong, Y.-S. Zheng and B. Z. Tang, Chem. Soc. Rev. 47 (2018) 7452.

[4] D. D. La, S. V. Bhosale, L. A. Jones and S. V. Bhosale, ACS Appl. Mater. Interfaces 10 (2018) 12189.

[5] J. Mei, N. L. C. Leung, R. T. K. Kwok, J. W. Y. Lam and B. Z. Tang, Chem. Rev. 115 (2015) 11718.

[6] Z. Zhao, B. He and B. Z. Tang, Chem. Sci. 6 (2015) 5347..

[7] R. T. K. Kwok, C. W. T. Leung, J. W. Y. Lam and B. Z. Tang, Chem. Soc. Rev. 44 (2015) 4228.

[8] Y. Zhao, W. Wang, C. Gui, L. Fang, X. Zhang, S. Wang, S. Chen, H. Shi and B. Z. Tang, J. Mater. Chem. C 6 (2018) 2873.

[9] B. Huang, W. Chen, Z. Li, J. Zhang, W. Zhao, Y. Feng, B. Z. Tang, C. Lee, Angew. Chem. Int.

Ed. 57 (2018) 12473.

[10] Y. Kitagawa, M. Kumagai, T. Nakanishi, K. Fushimi, Y. Hasegawa, Dalton Trans. 49 (2020) 2431.

[11] Z. An, C. Zheng, Y. Tao, R. Chen, H. Shi, T. Chen, Z. Wan, H. Li, R. Deng, X. Liu and W. Huang, Nat. Mater. 14 (2015) 685.

[12] E. Lucenti, A. Forni, C. Botta, L. Carlucci, C. Giannini, D. Marinotto, A. Previtali, S. Righetto and E. Cariati, J. Phys. Chem. Lett. 8 (2017) 1894.

[13] Y. Y. Gong, G. Chen, Q. Peng, W. Z. Yuan, Y. J. Xie, S. H. Li, Y. M. Zhang and B. Z. Tang, Adv. Mater. 27 (2015) 6195.

[14] Kenry, C. Chen and B. Liu, Nat. Commun. 10 (2019) 2111.

[15] K. Yanagisawa, Y. Kitagawa, T. Nakanishi, T. Akama, M. Kobayashi, T. Seki, K. Fushimi, H. Ito, T. Taketsugu and Y. Hasegawa, Eur. J. Inorg. Chem. 2017 (2017) 3843.

[16] K. Yanagisawa, Y. Kitagawa, T. Nakanishi, T. Seki, K. Fushimi, H. Ito, and Y. Hasegawa, Chem. - Eur. J. 24 (2018) 1956.

[17] Y. C. Miranda, L. L. A. L. Pereira, J. H. P. Barbosa, H. F. Brito, M. C. F. C. Felinto, O. L. Malta, W. M. Faustino and E. E. S. Teotonio, Eur. J. Inorg. Chem. 2015 (2015) 3019.

[18] D. Casanova, M. Llunell, P. Alemany, S. Alvarez, Chem. Eur. J. 11 (2005) 1479.

[19] K. Binnemans, Coord. Chem. Rev. 295 (2015) 1.

[20] Y. Kitagawa, F. Suzue, T. Nakanishi, K. Fushimi, Y. Hasegawa, Dalton Trans. 47 (2018) 7327.

[21] Gd(III) complexes generally show the similar coordination geometry with that of Eu(III) complexes. Gd(III) ion also exhibit the higher emitting level than T_1 levels of general organic ligands. Based on these properties, Gd(III) complexes have been used to estimate T_1 levels of ligand moiety in Eu(III) complexes [22].

[22] M. Latva, H. Takalo, V. M. Mukkala, C. Matachescu, J. C. Rodriguez-Ubis, J. Kankare J. Lumin. 75 (1997) 149.

[23] G. F. de Sá, O. L. Malta, C. de Mello Donegá, A. M. Simas, R. L. Longo, P. A. Santa-Cruz, E. F. da Silva Coord. Chem. Rev. 196 (2000) 165.

[24] Y. Kitagawa, F. Suzue, T. Nakanishi, K. Fushimi, T. Seki, H. Ito, and Yasuchika Hasegawa, Commun. Chem. 3 (2020) 3.

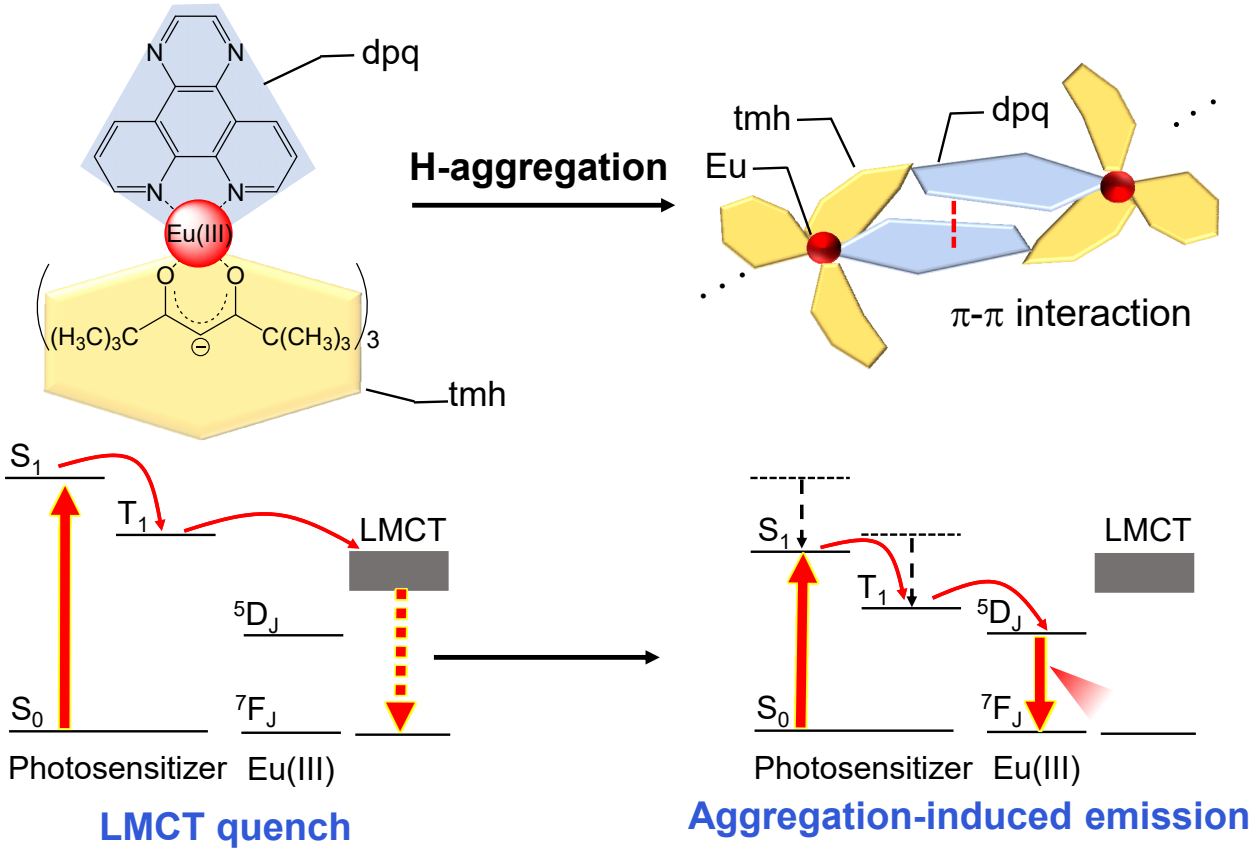

Figure 1. LMCT quenching and H-aggregation-induced emission for the Eu(tmh)$_3$dpq complex and its aggregates, respectively.

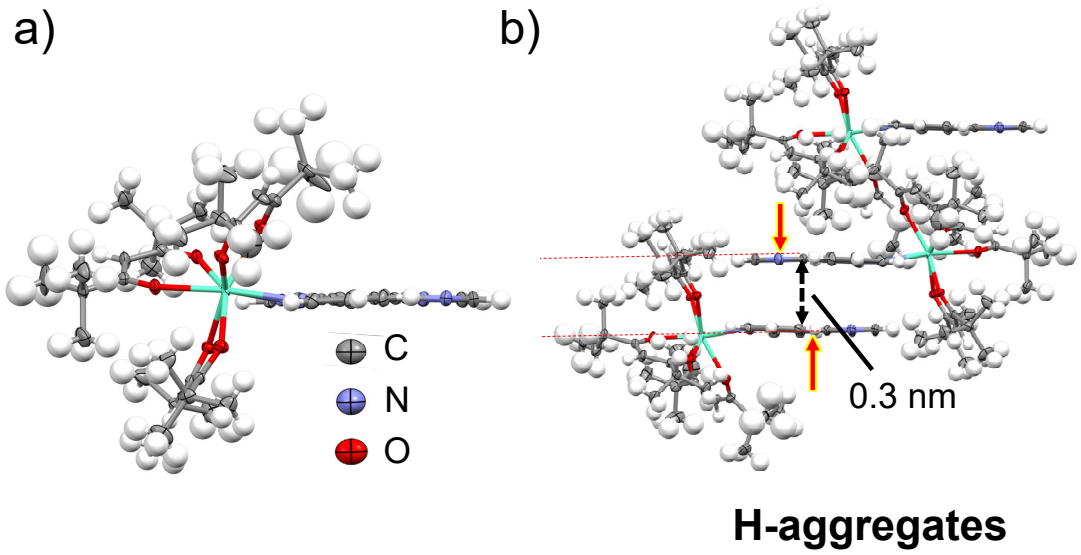

Figure 2. ORTEP drawings (thermal ellipsoids at 50% probability) of the X-ray crystal structures of a) one complex and b) the aggregate packing structure.

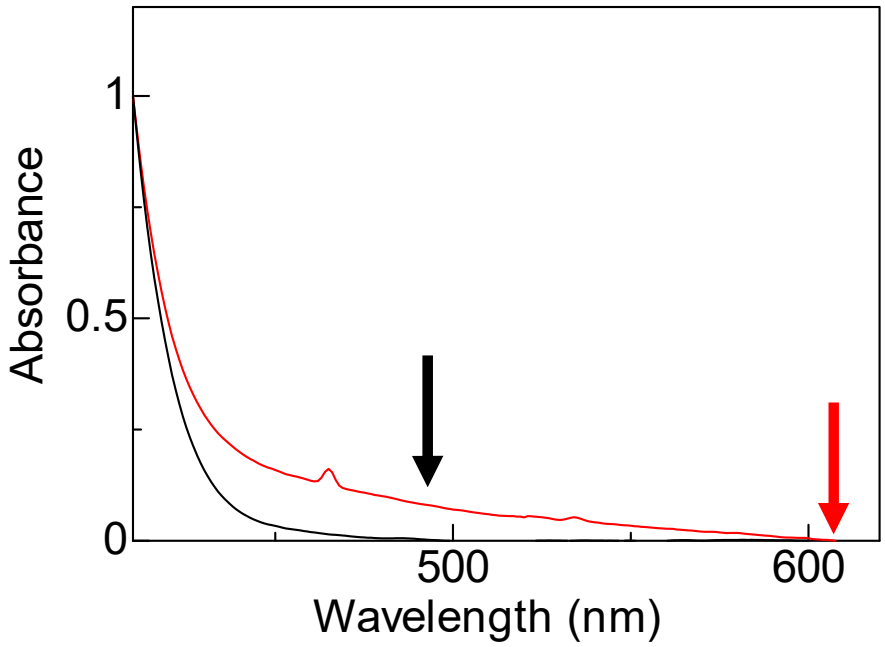

Figure 3. Electronic absorption spectra of $Tb(tmh)_3dpq$ (black line) and $Eu(tmh)_3dpq$ (red line) in CH_2Cl_2 (1.0×10^{-2} M). Arrows indicate absorption edge. Normalized by intensity maxima. The small absorption peaks at around 460 nm and 540 nm are attributed to $^7F_0 \rightarrow {}^5D_2$ and $^7F_1 \rightarrow {}^5D_1$ transitions, respectively [19].

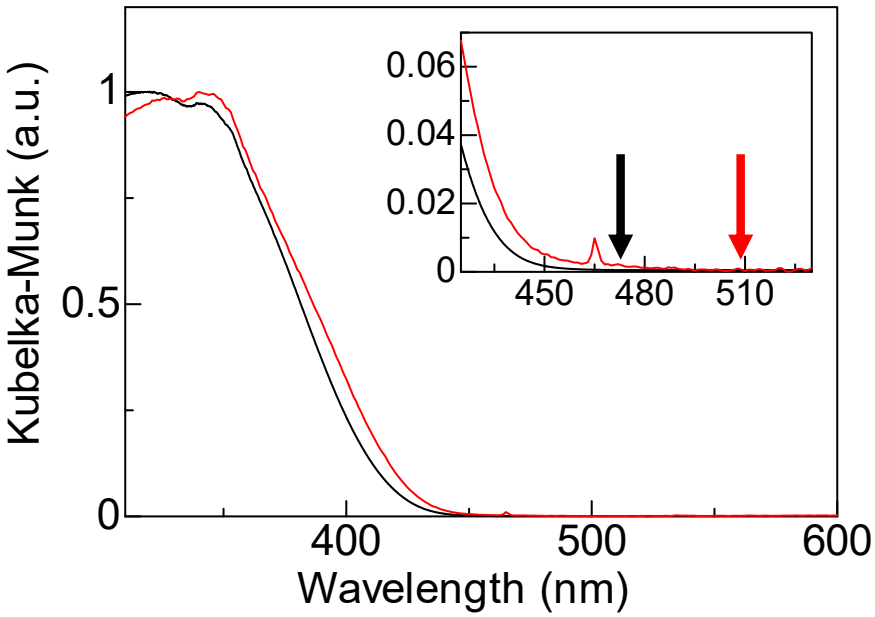

Figure 4. Diffusion reflectance spectra of $Tb(tmh)_3dpq$ (black line) and $Eu(tmh)_3dpq$ (red line) and in solid state. Arrows indicate absorption edge. Normalized by intensity maxima.

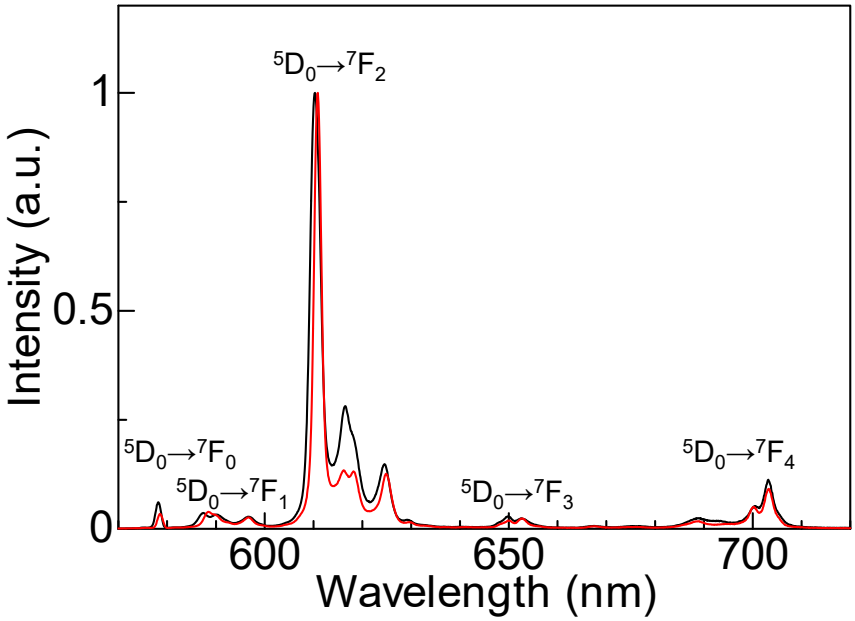

Figure 5. Emission spectra of $Eu(tmh)_3dpq$ in CH_2Cl_2 (5.0×10^{-2} M, black line) and in solid states (red line). Normalized by intensity maxima.

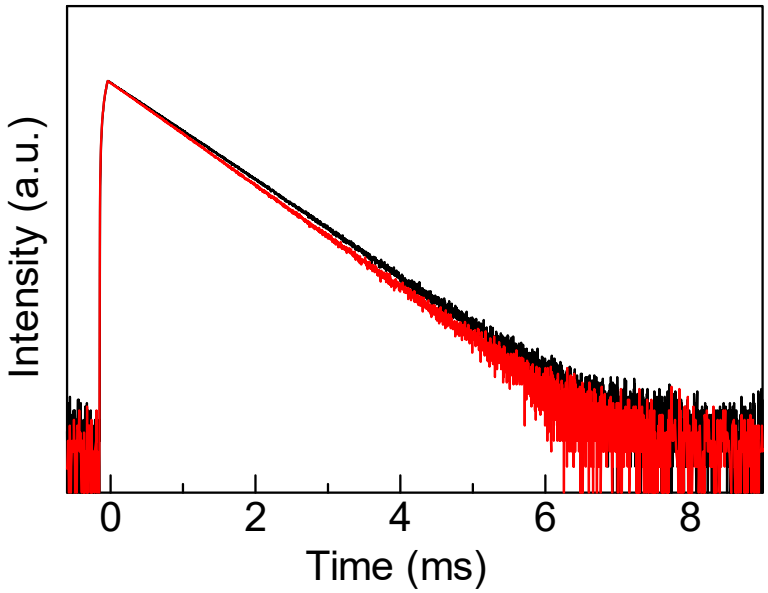

Figure 6. Emission decay curves of $Eu(tmh)_3dpq$ in CH_2Cl_2 (5.0×10^{-2} M, black line) and in solid states (red line).

Table 1. Photophysical properties of $Eu(tmh)_3(dpq)_2$

State	[a] τ_{obs} / ms	[b] k_r / s^{-1}	[b] k_{nr} / s^{-1}	Φ_{ff}	Φ_{tot}	η_{sens}
solution	0.76	8.0×10^2	5.2×10^2	61	[c] 1.2	2.0
solid	0.72	7.5×10^2	6.4×10^2	54	[d] 5.7	11

[a] τ_{obs} and Φ_{tot}: 5.0×10^{-2} M CH_2Cl_2 solution. [b] The Φ_{f-f}, k_r, and k_{nr} were calculated using equations. [c] λ_{ex} = 390 nm. [d] λ_{ex} = 410 nm.